行政院國家科學委員會專題研究計畫　期中進度報告

基地台所需之高崩潰電壓異質介面電晶體研究(1/2)

計畫類別：個別型計畫
計畫編號：NSC92-2215-E-009-058-
執行期間：92 年 08 月 01 日至 93 年 07 月 31 日
執行單位：國立交通大學電子工程學系

計畫主持人：李建平

計畫參與人員：廖志豪、李建騏

報告類型：精簡報告

處理方式：本計畫可公開查詢

中　華　民　國 93 年 6 月 6 日

行政院國家科學委員會專題研究計畫成果報告
基地台所需之高崩潰電壓異質介面電晶體研究(1/2)
High breakdown voltage HBTs for base station applications

計畫編號：NSC 92-2215-E-009-058
執行期限：92 年 8 月 1 日至 93 年 7 月 31 日

主持人：李建平教授　國立交通大學電子工程學系
計畫參與人員：廖志豪、李建騏　國立交通大學電子工程學系

一、中文摘要

高崩潰電壓電晶體現有兩主要技術，分別為高電壓砷化鎵電晶體及氮化鎵電晶體，我們進行了砷化鎵電晶體崩潰特性的模擬，及氮化鎵電晶體元件的製作，比較未摻雜(undoped)及調變摻雜(modulation-doped)結構氮化鎵異質結構場效電晶體的在不同溫度下的特性。氮化鎵元件結構對於元件在不同溫度下的特性有很大的影響。調變摻雜結構的元件在不同溫度下的特性都比未摻雜結構的元件要好。然而，未摻雜結構的元件特性對溫度的變化較小。

關鍵詞：氮化鎵、調變摻雜、砷化鎵異質介面電晶體、崩潰電壓

Abstract

There are tow main technologies that are the candidates of high breakdown voltage transistors for base station applications, i.e. high voltage GaAs HBTs and GaN HFETs. We are proceeding to do the simulations of GaAs HBTs breakdown behavior and the fabrications of GaN HFETs. A comparison on the device performance of the undoped and modulation-doped AlGaN/GaN HFETs over temperatures was presented. The results obtained indicated that the device structure has a significant influence on the device performance. The modulation-doped devices are superior to the undoped devices over the temperatures studied. The stability (the temperature dependence of device performance), however, is not as good as the undoped devices.

Keywords: GaN HFET, modulation-doped, GaAs HBT, breakdown voltage

I. Introduction

Compared with other technologies or material systems, InGaP/GaAs HBTs attract more attention as they start to dominate the huge field of power amplifier, especially in cellular phone application. In this project, we use 1-D simulator to simulate the breakdown IV curves. GaN heterostructure field effect transistors (HFETs) are promising candidates for high temperature and high power device applications at high frequencies due to their superior material properties [1]. For such operations, the stability of devices over temperature is extremely important. In addition to the commonly known problem in the thermal conductivity of substrates [2], the device structure plays a crucial role in realizing GaN-based HFETs for high temperature application. So far various device structures, such as the undoped structure [3], the modulation-doped structure [4] and the channel-doped structure [5], have been used to realize high performance GaN-based HFETs. Apparently devices with different structures may exhibit different electrical behaviors at high temperature due to their different transport properties. It is therefore desirable to understand which structure has better device performance at high temperature. In this work, a comparison on the high temperature performance of the undoped and modulation-doped AlGaN/GaN HFETs is reported. The results obtained indicate that device structure has a significant influence on the device high temperature

performance. The modulation-doped devices, with a higher electron concentration, comparable mobility and lower parasitic source resistance at high temperatures, exhibited better dc and RF performance than the undoped devices over temperatures.

II. Method

Two structures, one undoped structure and one modulation-doped structure, were grown by metalorganic chemical vapor deposition (MOCVD) on c-plane sapphire substrates. The undoped structure consists of a 3 μm undoped GaN buffer layer and a 28 nm undoped AlGaN layer. The modulation-doped structure consists of a 3 μm undoped GaN buffer layer, a 3 nm undoped AlGaN spacer, a 20 nm Si-doped AlGaN with a doping concentration of 5×10^{18} cm^{-3} and a 5 nm undoped AlGaN cap layer. The Al composition is 0.3 for all AlGaN layers. After layer growth, mesa patterns for device active regions were defined by photolithography. Excellent ohmic contacts using contact metal, Ti/Al/Ti/Au (200/1500/450/550 Å) were obtained after the samples were annealed at 750°C for 30 s in N_2 gas ambient. Contact resistances of 0.59 ohm-mm for the undoped devices and of 0.38 ohm-mm for the modulation doped devices were obtained. The source-drain spacing is 2 μm for all samples. T-shaped gates using Ni/Au (20/300 nm) were then formed to complete the FET fabrication.

At room temperature, the Hall measurement results showed that the undoped structure had an electron concentration of 1×10^{13} cm^{-2} and a mobility of 1100 cm^2/Vs. The modulation-doped structure had an electron concentration of 1.23×10^{13} cm^{-2} and a mobility of 953 cm^2/Vs. The sheet electron concentration for the undoped structure was independent of temperature even when the temperature was raised to 500K. For the modulation doped structure, however, the sheet carrier density increased to 1.33×10^{13} cm^{-2} at 500K. The electron mobility decreased at high temperatures. At 500K the values were 537 cm^2/Vs and 529 cm^2/Vs for the undoped structure and the modulation doped structure, respectively.

For HBT simulations, the low field mobility formulas are taken from Sotoodeh's work [6]. The recombination parameters are selected as follow: Copt = 1 x 10^{-11} cm^3s^{-1}, Cn = 7 x 10^{-30} cm^6s^{-1}, Cp = 1 x 10^{-30} cm^6s^{-1}, τn = 2.9 x 10^{-6} s, and τp = 5 x 10^{-8} s for GaAs; Copt = 1 x 10^{-10} cm^3s^{-1}, Cn = 3 x 10^{-30} cm^6s^{-1}, Cp = 3 x 10^{-30} cm^6s^{-1}, τn = 2 x 10^{-9} s, and τp = 2 x 10^{-9} s for InGaP, where Copt is radiative recombination coefficient, Cn is electron Auger recombination coefficient, Cp is hole Auger recombination coefficient, τn is electron SRH lifetime, and τp is hole SRH lifetime. The GaAs effective mass and band gap data are taken from Blakemore's paper [7]. For InGaP, the electron effective mass is taken to be 0.088 [8], the temperature dependent band gap relation are obtained by fitting Ishitani's PL data [9] as,

$$E_{g,InGaP} = 1.985 - 7.19\times10^{-4}\frac{T^2}{T+482} \quad (1)$$

Other data are from Brennan's work [10].

We take band gap narrowing (BGN) into account for GaAs by using Luo's data [11] for n-type GaAs BGN and Harmon's [12] for p-type GaAs BGN. Those are,

$$\Delta E_{gp} = 2.55\times10^{-8} p^{\frac{1}{3}} \quad (2)$$

$$\Delta E_{gn} = 3.60\times10^{-8} n^{\frac{1}{3}} \quad (3).$$

Because different regions have different doping and different ΔEg, every junction grid point must be treated as a heterojunction, and we choose ΔEc = 0.5ΔEg. As all junctions having band offset, we use thermionic emission boundary conditions based on the theory by Wu and Yang [13] to calculate the quasi-Fermi level splitting at junction. Additionally, we follow Blakemore's formulation [7] to simulate the non-parabolic effect and re-formulate thermionic emission with non-parabolic effect in heavily doped degenerate regions, like base, to see the influence on band offset.

Our devices are single heterojunction InGaP HBT (SHBT) grown by metal–organic chemical vapor deposi-tion (MOCVD). The

epitaxial structure consists of a Si-doped ($3\times10^{17}cm^{-3}$) 400 Å In0.49Ga0.54P emitter, a car-bon-doped ($4\times10^{19}cm^{-3}$) 1200 Å GaAs base, and a Si-doped ($1\times10^{16}cm^{-3}$) 1-mm GaAs collector. The emitter cap and sub-collector are both heavily doped. Finally, devices cover with SiN for passivation.

The simulation code uses the finite difference relaxation method [14] to solve the Poisson equation, the electron current continuity equation, and the hole current continuity equation together with different converge requirement.

III. Result and discussion

Devices with a gate dimension of 0.15 μm (gate length) by 75 μm (width) were used for this study. Both devices showed good dc performance over the whole measured temperature range. The threshold voltages at room temperature were around –7 V and –9 V for the undoped and the modulation doped devices. Figure 1 shows the comparison of the temperature dependence of the maximum drain current at a gate bias V_{gs}= 2 V. The undoped device showed the maximum drain current of 700 mA/mm at room temperature. At 200°C it reduced to 567 mA/mm. The modulation-doped device exhibited a larger maximum drain current. At room temperature, it was of 1040 mA/mm and at 200°C it became 678 mA/mm. The larger change in the maximum drain current for the modulation-doped device can be attributed to the temperature dependent sheet carrier density.

Figure 2 shows the comparison of the maximum extrinsic transconductances measured at a drain bias V_{ds}= 5 V for both devices over temperature. In general, the modulation-doped devices had a higher transconductance than the undoped devices. But the undoped device had a smaller change in transconductance over temperature. For the modulation doped structure, the transconductance changed from 198 mS/mm at room temperature to 125 mS/mm at 200°C. For the undoped device, the transconductances ranged from 113 mS/mm to 86 mS/mm over the temperatures. The lower transconductance is due to the large source resistance, which was 3.4 ohm-mm, of the undoped channel in the undoped device. For the modulation-doped device it was 2.67 ohm-mm.

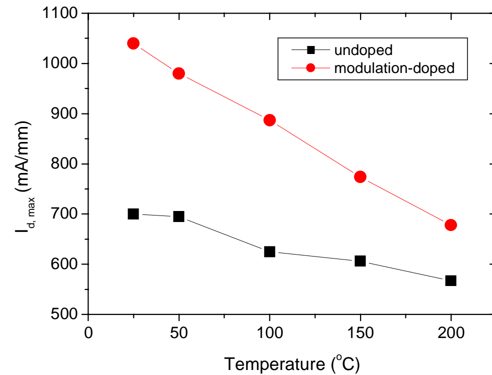

Figure 1. Temperature dependence of the maximum drain current of the undoped and modulation-doped devices.

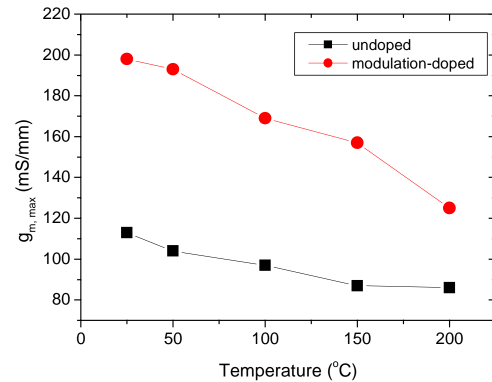

Figure 2. Temperature dependence of the maximum extrinsic transconductance of the undoped and modulation-doped devices.

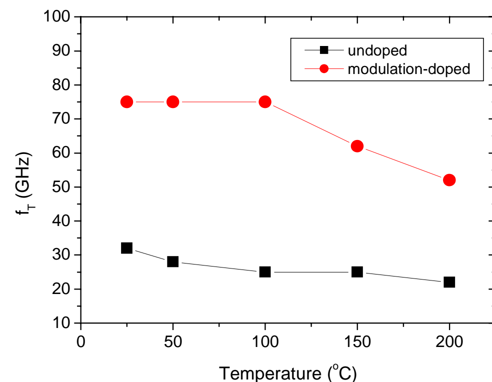

Figure 3. Temperature dependence of current gain cut-off frequency of the undoped and modulation-doped devices.

Figure 3 shows the comparison of the temperature dependence of the current gain cut-off frequency (f_T) for both devices. The undoped device was operated at V_{ds}= 6 V and V_{gs}= -3.5 V. The modulation-doped device

was operated at V_{ds}= 6 V and V_{gs}= -6 V. For the undoped device, the cut-off frequency was 32 GHz at room temperature, but degraded to 22 GHz at 200°C. The modulation-doped device had a room temperature f_T of 75 GHz and did not show obvious degradation until 100°C. Above 100°C, the cut-off frequency became lower and dropped to 52 GHz at 200°C. As a whole, both devices did not show obvious degradation for temperatures below 100°C. Similar results were also observed in the doped channel AlGaN/GaN HFETs [5]. The main reason is the weak temperature dependence of electron transport property [15-16]. The lower cut-off frequency for the undoped device is mainly attributed to the larger parasitic source and drain resistances.

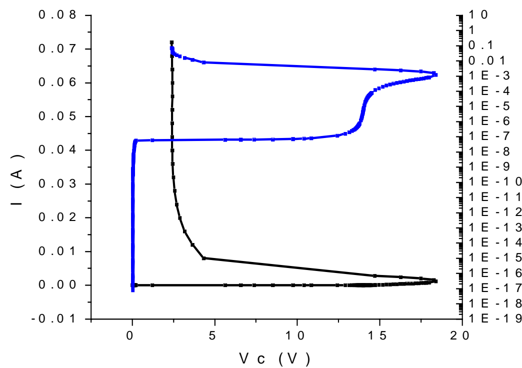

Figure 4. The simulated breakdown IV curves at $I_B = 1\times10^{-2}\,\text{A/cm}^2$.

Based on the Hall measurement results, the undoped device had a constant two-dimensional electron gas (2DEG) concentration in the channel over a wide temperature range. The modulation-doped device had a higher electron concentration but it increased with temperature, due to the thermal activation of Si donors in the AlGaN layer [17]. Although lower electron mobility was observed in the modulation doped devices due to the additional ionized impurity scattering associated with the Si donors, the electron mobilities for both devices are similar at high temperatures where phonon scattering is the dominant scattering process [18]. Because of the additional doping, the modulation-doped devices has lower parasitic source and drain resistances than the undoped devices over temperatures. Putting all these factors together, we may conclude that the modulation-doped devices are superior to the undoped devices over the temperatures studied. The stability (the temperature dependence of device performance), however, is not as good as the undoped devices.

Figure 4 shows the simulated breakdown IV curves at $I_B = 1\times10^{-2}\,\text{A/cm}^2$. The measured breakdown voltage is about 16V. The simulation and the measurement are quit fitted.

IV. Conclusion

We have compared the performance of the undoped and modulation-doped AlGaN/GaN HFETs over temperatures. The results obtained indicate that the device structure has a great influence on the device performance. The modulation-doped devices are superior to the undoped devices over the temperatures studied. The stability (the temperature dependence of device performance), however, is not as good as the undoped devices. A 1-D HBT simulator is constructed. We could use it to design a high breakdown HBT.

References

[1] L. F. Eastman *et al.*, IEEE spectrum, **May**, p.28 (2002).

[2] R. Gaska *et al.*, IEDM Tech. Dig., p.565 (1997)

[3] L. F. Eastman *et al.*, IEEE Trans. Electron Devices, **48**, p.479 (2001).

[4] M. Akita *et al.*, IEEE Electron Device Lett., **22**, p.376 (2001).

[5] Q. Chen *et al.*, Electron Lett., **33**, p.637 (1997).

[6] M. Sotoodeh, A. H. Khalid, and A. A. Rezazadeh , J. Appl. Phys. **87** (2000) 2890.

[7] J. S. Blakemore, J. Appl. Phys. **53** (1982) R123.

[8] P. Emanuelsson, M. Drechsler, D. M. Hofmann, B. K. Meyer, M. Moser and F. Scholz, Appl. Phys. Lett. **64** (1994) 2849.

[9] Y. Ishitani, S. Minagawa, and T. Tanaka, J. Appl. Phys. **75** (1994) 5326.

[10] K. F. Brennan and P.-K. Chianga , J. Appl. Phys. **71** (1992) 1055.

[11] H.T. Luo, W.Z. Shen, Y.H. Zhang, H.F.Yang, Phys. B **324** (2002) 379.

[12] E. S. Harmon, M. R. Melloch, and M. S. Lundstrom, Appl. Phys. Lett. **64** (1994) 502.

[13] C. M. Wu and E. S. Yang, Solid-State Electron. **22** (1979) 241.

[14] W. H. Press, S. A. Teukolsky, W. T. Vetterling, and B.P. Flannery, *Numerical Recipes in C++* (2002).

[15] N. S. Mansour *et al.*, J. Appl. Phys., **77**, p.2834

(1995).
[16] U. V. Bhapkar *et al*., J. Appl. Phys., **82**, p.1649 (1997).
[17] C. C. Lee *et al*., Jpn. J. Appl. Phys., **43**, P.L740 (2004)
[18] N. Maeda *et al*., Appl. Phys. Lett., **79**, p.1634 (2000).

行政院國家科學委員會補助專題研究計畫 □成果報告 ☑期中進度報告

基地台所需之高崩潰電壓異質介面電晶體研究(1/2)

計畫類別：☑ 個別型計畫　　□ 整合型計畫
計畫編號：NSC 92－2215－E－009－058－
執行期間：92 年 8 月 1 日至 93 年 7 月 31 日

計畫主持人：李建平
共同主持人：
計畫參與人員：廖志豪、李建騏

成果報告類型(依經費核定清單規定繳交)：☑精簡報告　□完整報告

本成果報告包括以下應繳交之附件：
□赴國外出差或研習心得報告一份
□赴大陸地區出差或研習心得報告一份
□出席國際學術會議心得報告及發表之論文各一份
□國際合作研究計畫國外研究報告書一份

處理方式：除產學合作研究計畫、提升產業技術及人才培育研究計畫、列管計畫及下列情形者外，得立即公開查詢
□涉及專利或其他智慧財產權，□一年□二年後可公開查詢

執行單位：國立交通大學電子工程學系

中　華　民　國　93　年　5　月　31　日